Ultra Wideband Multiple Resonant Transducer

John L. Butler and Alexander L. Butler,
Image Acoustics, Inc., Cohasset, MA 02025
jbutler@imageacoustics.com

Abstract- **Tonpliz piston transducers are generally operated in the vicinity of their fundamental resonance while operation above resonance is usually required for wider band performance. However, this wide band performance is often limited by nulls in the response due to cancellation between the modes of vibration and the inability of the drive system to perform at these null frequencies. The Multiple Resonant (MR) transducer concept avoids these problems and excites a large number of extensional resonant modes of a distributed transducer system in a way, which allows addition between these modes [1]. Our approach uses a distributed transmission line transducer with the transduction elements specifically situated to excite *both* odd and even numbered modes (1, 2, 3, etc.), accomplishing in-phase addition between modes. Wide bandwidth is obtained by excitation of all the modes up to the frequency at which the active transduction element is one wavelength long. Feedback control is used to smooth the response and provide velocity control under interactive array steered conditions. (Work supported by a Phase II SBIR from ONR.).**

I. INTRODUCTION

Normally electro-acoustic underwater transducers are operated in the vicinity of the fundamental resonant frequency. Maximum output is obtained at the resonant frequency; however, operation in the vicinity of this frequency limits the bandwidth of the transducer. Wideband performance can be obtained above resonance but the band is often limited by the next overtone resonance. Because of phase shifts, the presence of this overtone resonance generally creates a cancellation between the two resonant frequencies typically resulting in a significant reduction, or notch, in the level of the response, thus limiting the bandwidth.

Part of the difficulty is due to unwanted lateral modes of vibration of the driving stack as well as flexural modes of vibration of the piston radiator. With these under control, however, there is still a major wideband impediment due to the cancellation between overtone modes. This cancellation is due to the 180 degree phase shift between the mass controlled region of the lower resonance and the stiffness controlled region of the next upper resonance. We will show that this resulting notch may be eliminated through the introduction of an additional phase shifted resonance between these modes. This introduction of an additional resonant frequency allows a distribution of the coupling coefficient over the band of operation and improves transducer power factor. We will also show that feedback may be used to control the output velocity and improve the response under single element and array interactive conditions. Results on the MR40 transducer design, which operates in the 10 kHz to 40 kHz band and incorporates the multiple resonant features as well as feedback control, will be presented.

II. WIDEBAND OPERATION THEORY

The operation of the transducer may be understood by referring to Figs. 1a, 1b, 1c and 1d which illustrate the physical models and Figs. 2a through 2d which illustrate the calculated resulting acoustic pressure amplitude and phase response. Fig. 1a illustrates a piezoelectric longitudinal bar resonator operating in the piezoelectric 33-mode and composed of four separate piezoelectric elements wired in parallel and polarized, as shown by arrows for additive motion in the longitudinal direction. The dashed lines illustrate the symmetrical displacement of the bar for a voltage +V. The fundamental resonance occurs when the bar is one-half wavelength long and the next harmonic occurs when the bar is one wavelength long, but this cannot be excited by the voltage arrangement of Fig. 1a. Because of the electrical symmetry, only the first half-wavelength fundamental resonance and all the odd harmonics are excited, but not the even harmonics. If f_1 is the fundamental half wavelength resonance, then the odd harmonic frequencies are $f_{2n-1} = (2n - 1)f_1$ for n = 1, 2, 3, …. The amplitude response of the acoustic pressure to the right of

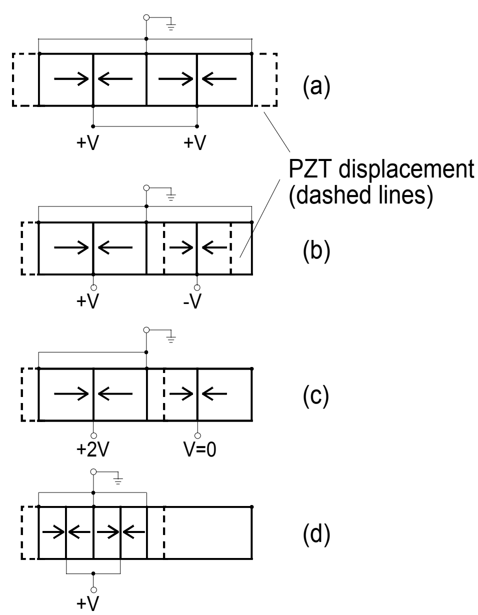

FIG. 1 Physical models illustrating the operation of the transducer

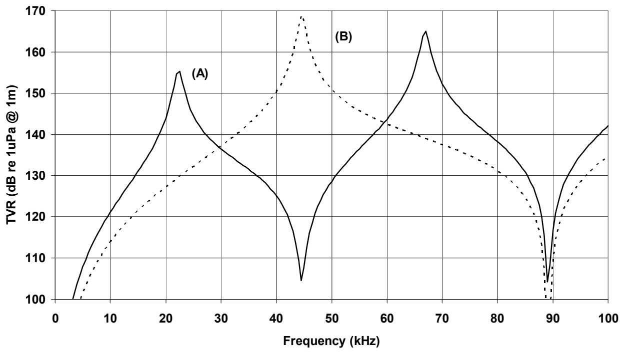

FIG. 2a

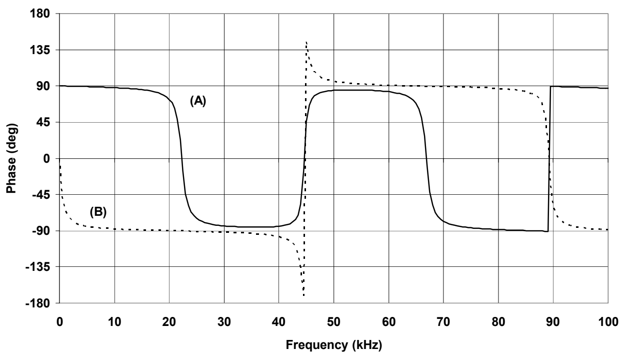

FIG. 2b

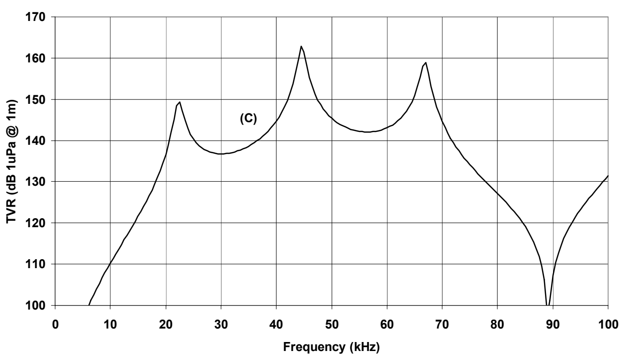

FIG. 2c

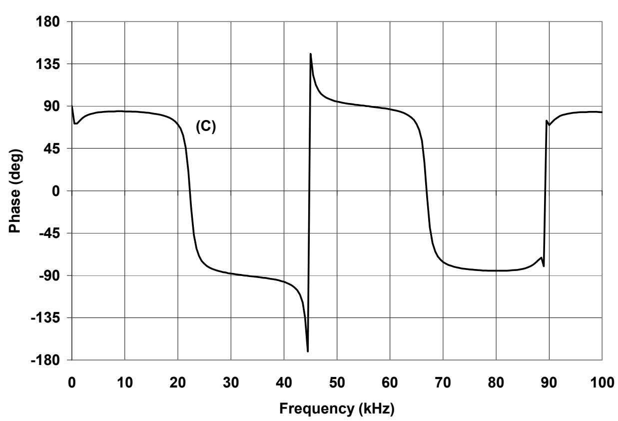

FIG. 2d

FIG. 2 The calculated resulting acoustic pressure amplitude and phase response of the physical models in figure 1.

the bar is shown in Fig. 2a by the curve labeled (A) showing a fundamental resonance at 22.5 kHz and a third harmonic resonance at 67.5 kHz and a strong null at 45 kHz which is also the frequency of the second harmonic, but cannot be excited by the arrangement of Fig. 1a. The null at approximately 45 kHz is particularly deep because the phase of the mass controlled region of the fundamental is 180 degrees out of phase with the phase of the stiffness controlled region of the third harmonic resonant leading to a cancellation. The occurrences of these nulls limit the usefulness of such a system to provide a wideband response. The multiple resonant, MR, concept provides a means and method for adding a resonant response at these nulls in a constructive way using the even harmonics.

The even harmonics (but not the odd) are excited by the arrangement of Fig. 1b where the polarity of the voltage, V, on the right hand pair of elements is reversed. This causes a contraction on the right element pair while the left element pair expands. This is illustrated in Fig. 1b by the dashed lines. The excited even harmonic resonances are given by $f_{2n} = (2n)f_1$ for n = 1, 2, 3, …. The first even harmonic acoustic pressure amplitude response is plotted as curve (B) in Fig. 2a and seen to resonate at approximately 45 kHz which is just the location of the null for the wiring arrangement of Fig. 1a. The even harmonic motion on the right side of the bar is 180 degrees out of phase with the first odd harmonic mode as may readily be seen by comparing the displacements of Fig. 1a with the displacements of Fig. 1b. The corresponding phase response is illustrated in Fig. 2b showing out of phase nature at low and high frequencies but in-phase motion at mid frequencies from 30 kHz to 60 kHz. It is because of the additional phase shift of Figs. 1a and 1b that yields the ultimate in-phase condition at mid band which allows the constructive addition of the even harmonics of Fig. 1b to the odd harmonics of Fig. 1a if the two systems are added.

The sum of the voltage conditions of Figs. 1a and 1b leads to the condition illustrated in Fig. 1c showing 2V volts on the left piezoelectric pair and 0 volts on the right piezoelectric pair. Since the V = 0 voltage drive section is no longer active in generating a displacement it may be replaced by the electrically inactive transmission line as shown in Fig. 1d. (Also shown in Fig. 1d is a reconfigured drive section with elements of half thickness for the same strain as Fig. 1c but with 1 volt drive as in Figs. 1a and 1b.) The wideband acoustic pressure amplitude response for the cases of Fig. 1c or 1d are given in Fig. 2c showing the addition of the even harmonic resonance at 45 kHz filling in the original null with no nulls between the resonances as desired. The resulting phase response, shown in Fig. 2d, is a selective result of the two phase curves of Fig. 2b as determined by the amplitude of the corresponding harmonic response of Fig. 2c. The harmonic frequencies for this case are $f_n = (n)f_1$ for n = 1, 2, 3, …. The first null now appears in the vicinity of 90 kHz at twice the frequency of the 45 kHz null for the original case of Fig. 1a and thus doubling the bandwidth. This null occurs when the left hand piezoelectric pair is one wavelength long. The transducer now resonates in its fundamental mode, its second harmonic mode and its third harmonic. The bandwidth can be increased by reducing the proportional length of the active piezoelectric section allowing the excitation of higher harmonic modes such as the fourth, fifth and sixth modes, thus allowing an ultra wide bandwidth.

This method provides a means for the addition of both odd and even modes yielding a wideband response of multiple resonances without destructive interference which would result in nulls. Each mode has an associated electromechanical coupling coefficient allowing a distribution of coupling over the frequency band improving the wideband effective electromechanical coupling coefficient of the transducer.

III. FEEDBACK CONTROL

Feedback control provides a smoother response and also yields array control by fixing the velocity of the pistons through out the array. Feedback causes the voltage to maintain a constant velocity of the piezoelectric element in the vicinity of the junction between the transmission line and the piezoelectric stack. One way of understanding this is to consider the simplified case of velocity feedback for a lumped system of mass M, stiffness K, resistance R and drive force F given by $N(V + V_f)$ where V is the drive voltage, V_f, is the feedback voltage and N is the electro mechanical turns ratio for the transducer. The equation of motion may be written for the displacement, x, as

$$Md^2x/dt^2 + Rdx/dt + Kx = N(V + V_f) \quad (1)$$

The case with no feedback is for $V_f = 0$. With the feedback voltage proportional to the velocity and written as $V_f = -Adx/dt$ we get

$$Md^2x/dt^2 + (R + NA)dx/dt + Kx = NV \quad (2)$$

It can be seen that the self-resistance, R, appears to be increased by an amount NA increasing the value of the total self-resistance, reducing the value of the mechanical $Q_m = \omega M/(R + NA)$ through the additional “virtual resistance”, NA, in the denominator.

Under array loading conditions the mutual interaction impedance will have less effect on the velocity response under feedback control. This is particularly important in the lower frequency range where the self-impedance is small and the mutual impedance is significant. Under sinusoidal conditions with R_m the mutual radiation resistance, the solution for the velocity, u, may be written as

$$u = NV/[j(\omega M - K/\omega) + R + R_m + AN] \quad (3)$$

and for A very large so that $AN >> R_m + R$, in the vicinity of resonance we get a constant velocity $u \approx V/A$. This is an extreme and ideal case of feedback but a case, which illustrates the velocity conditions, which are approached as the negative feedback gain is increased.

One means for reducing unwanted positive feedback at higher frequencies is to place the sensor at a location, which is insensitive to unwanted higher order resonant modes. The piezoelectric sensor generates a voltage that is proportional to the compression. Waves traveling along the stack produce standing waves at corresponding resonant frequencies and are characterized by a stress and displacement distribution. Nulls in the stress occur at peaks in the displacement. Thus, placement of the sensor at the location of the displacement peak(s) will yield minimal output for those modes. We have done just that with the MR40 and chosen a location, which yields high output at the desired fundamental 24 kHz resonant mode but yields little output in the vicinity of unwanted modes. This was possible by inspection of the displacement modes of vibration on our finite element model.

IV. FINITE ELEMENT AND ARRAY MODELING

The operation of the transducer was considered for a thirty-six element closely packed array configuration. Transducer A,B,C,D results were obtained from our finite element model and used in the program ARRAY [2] to obtain array results including the steered beam patterns, element velocities and array radiation resistances. The feedback cases used two additional parameters to include the feedback sensor. The transducer equation set for the input voltage E, current , I, force, F, velocity, u, and feedback voltage, E_f, may be written as

$$E = AF + Bu \quad (4)$$

$$I = CF + Du \quad (5)$$

$$E_f = GF + Hu \quad (6)$$

where the coefficients G and H describe the voltage performance of the feedback sensor. With, K, the gain of the feedback amplifier, voltage inverter and integrator we can now write the summed voltage, $E_s = E + KE_f$, at the transducer as

$$E_s = (A + KG)F + (B + KH)\, u \quad (7)$$

The new equation “A,B,C,D” set may then be written as

$$E_s = A_sF + B_su \quad (8)$$

$$I = C\,F + D\,u \quad (9)$$

where the new “A” and “B” parameters, A_s and B_s, include the summed feedback signal and are given by $A_s = A + KG$ and $B_s = B + KH$. These finite element A_s, B_s, C, D values were used in the program ARRAY to evaluate the single element and array performance of the transducer. A circuit analysis model, with feedback, was also developed and used as a tool for more rapid evaluation during optimization.

V. MR40 TRANSDUCER AND ARRAY DESIGN

An extremely wide band transducer, the MR85, was initially investigated before the development of the MR40 transducer. A sketch of the MR85 with a Lucite transmission line is shown in Fig. 3.

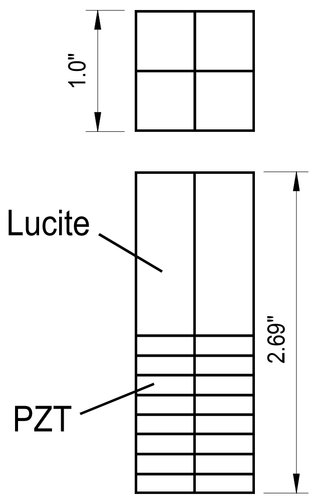

FIG. 3 Ultra Wideband MR85 four-element module

The circuit analysis results without and with ideal velocity feedback are shown in Fig. 4. As seen, the multiple resonant frequencies have no nulls between them and the feedback yields a reasonably smooth response over a band of three octaves. The coupling coefficients at the first five resonances were found to be 0.20, 0.29, 0.60, 0.65 and 0.20. The piezoelectric stack is one wavelength long at 90 kHz creating a null at this frequency.

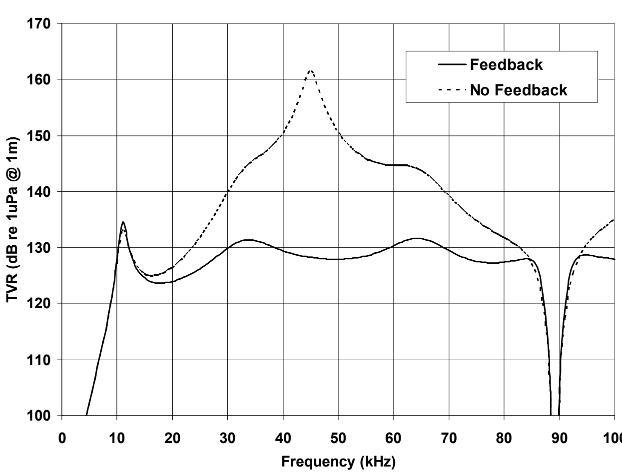

Fig. 4 The circuit analysis transmitting voltage response without and with ideal velocity feedback.

Although these results were encouraging and substantiated our concept, we focused our attention on a narrower two-octave 10 kHz to 40 kHz band MR40 design where there was systems interest and where feedback control was less formidable. The MR40 was designed for a surface intensity of at least 5 w/cm^2.

FIG. 5 Fabricated MR40 single element transducer

A photograph of the MR40 transducer is shown in Fig. 5. The piston diameter is 1.2 inches and the overall length is 4 inches. A GRP transmission line is used between the piezoelectric stack and the piston head. The stack is sandwiched between a tungsten tail mass and a steel plate which interfaces to the GRP. A compression stress rod is screwed from the tail into the steel plate. The piezoelectric stack is assembled from ten rings operated in the 33 mode along with a small piezoelectric sensor ring for feedback control. A sketch of the transducer and feedback system is shown in Fig. 6. The sensor output is proportional to the stress which is integrated and subtracted from the input signal.

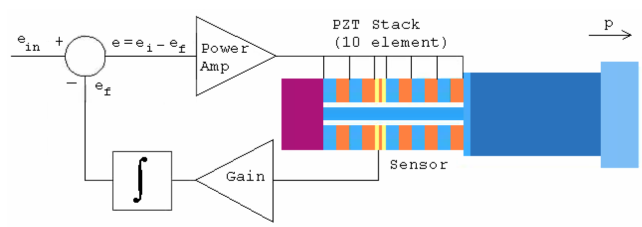

FIG. 6 MR40 feedback system

The location of the sensor was determined from a finite element analysis [3] of the stress distribution for the modes of interest. It was positioned for minimum output from unwanted positive feedback from higher order modes, yet sensitive to the desired fundamental modes. The modal displacement of the first three modes of vibration is shown in Fig. 7 at 11.4, 24.2 and 40.4 kHz for the 1^{st}, 2^{nd} and 3^{rd} overtone modes. These are not exact harmonics because of the head and tail masses and the lateral GRP motion at 40.4

kHz. Finite element TVR results without and with feedback are shown in Fig. 8 showing a 16 dB suppression of the strong mid band resonance.

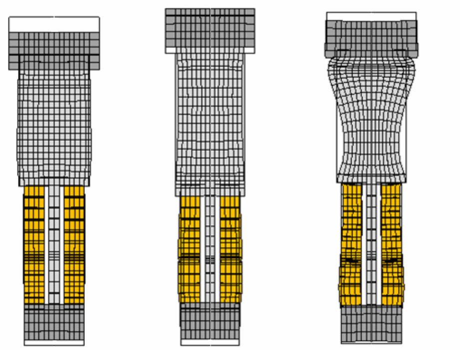

FIG. 7 The modal displacement of the first three modes of vibration at 11.4, 24.2 and 40.4 kHz for the 1st, 2nd and 3rd overtone modes

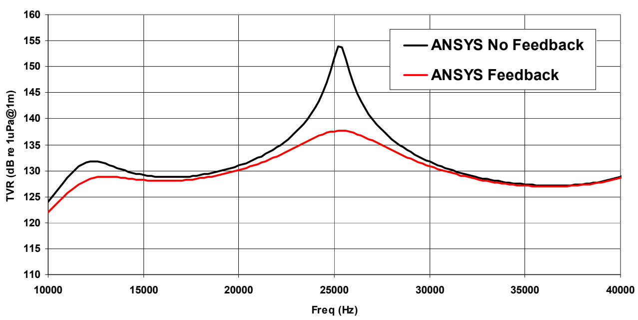

FIG. 8 Finite element transmitting voltage response without and with feedback

Additional computer models were used to analyze the design under single element and array conditions. The program TRN [4] was used to evaluate the velocity distribution of an array of sixty-four MR40 elements steered to 60 degrees at 25 kHz. The results shown in Fig. 9 demonstrate the importance of feedback in maintaining a nearly uniform velocity, particularly under steered conditions.

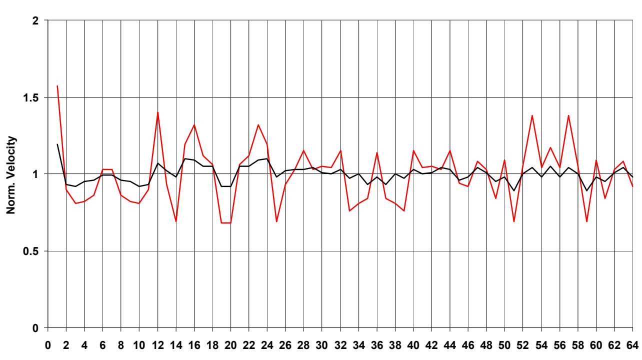

FIG. 9 Example of array velocity distribution steered 60°. Red curve is a conventional Tonpilz and the balck curve is the MR40 with feedback.

The transducer was also analyzed using the transducer circuit analysis program TAP [5] and compared with measurements. A comparison of the corresponding calculated and measured in-air impedance magnitude is shown in Fig. 10 and a comparison with resonance, f_r, anti resonance, $f_{a,}$ and effective coupling coefficient, k, is shown in Table I.

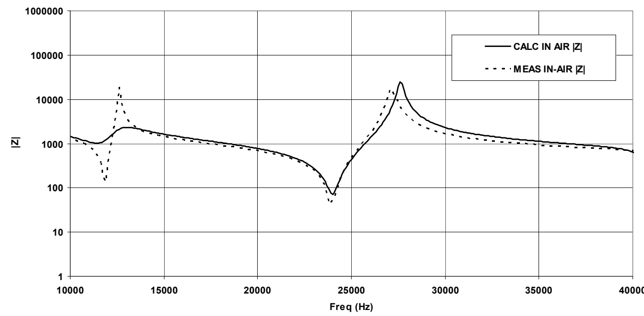

FIG. 10 Single element in-air measured impedance magnitude

TABLE I Single element in-air calculated and measured results

	f_{r1} (kHz)	f_{a1} (kHz)	k_1	f_{r2} (kHz)	f_{a2} (kHz)	k_2
Circuit Analysis	11.8	12.6	0.35	24	27.6	0.49
Measured	11.91	12.62	0.33	23.84	27.08	0.47

The single element in-water results without and with feedback are shown in Figs. 11 and 12 respectively. The results were encouraging enough to fabricate and evaluate an array of thirty-six MR40 elements.

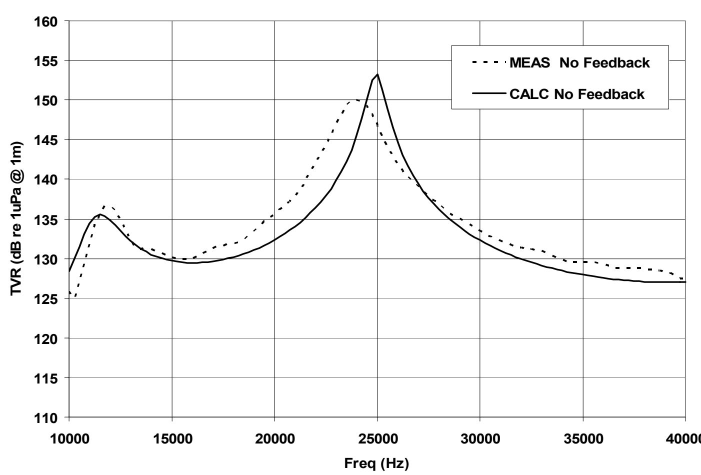

FIG. 11 Single element in-water measured transmitting voltage response without feedback.

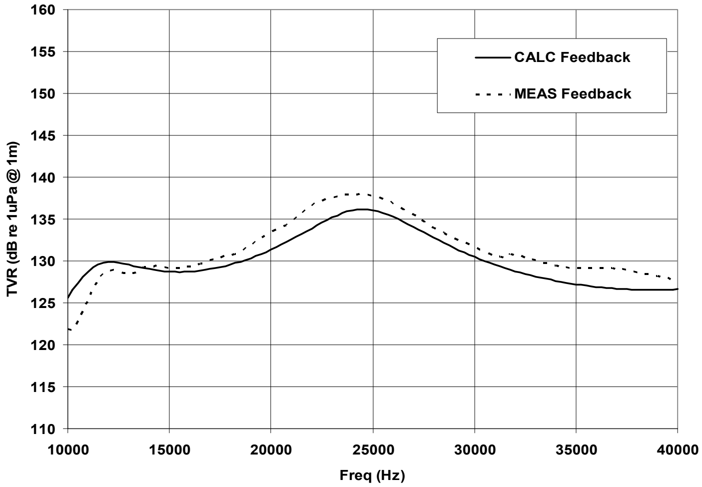

FIG. 12 Single element in-water measured transmitting voltage response with feedback.

FIG. 13 Thirty-six element staggered array.

The thirty six element staggered array is shown in the photograph of Fig. 13. The six-element columns were staggered to reduce the center-to-center effective element spacing from 1.2 inches to 1.1 inches. The array was wired in parallel for initial testing of its performance without and with feedback. These results are compared with calculated results in Figs. 14 and 15. As seen, in Fig. 14 the array mounting introduced damping at the mid band resonance showing a deviation from the original model in the vicinity of that resonance. However, as seen, the agreement is quite good above and below that resonance. This a common situation in which the damping value, due to mounting, is difficult to anticipate until measurements have been made. Good agreement is seen in Fig. 15 for the case of feedback control. Although not shown here, the transducer was additionally analyzed and shown to be capable of hydrophone performance without and with feedback. The array should be capable of a minimum source level of 220 dB from 10 kHz to 40 kHz for an electric field drive at 7,500 volts/inch.

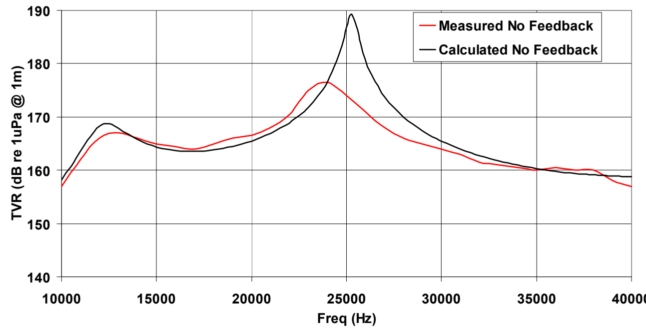

Fig. 14 Measure and calculated array transmitting voltage response without feedback.

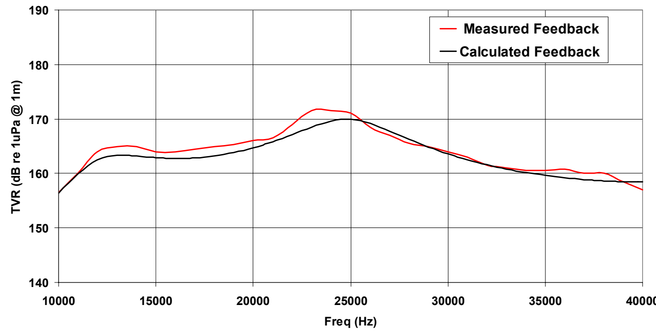

Fig. 15 Measure and calculated array transmitting voltage response with feedback.

VI. CONCLUSIONS

A consecutive mode method for achieving wide transducer bandwidth as well as a method for feedback control has been described. It was shown that the feedback control scheme provides a smooth transducer response over a wide band and stabilizes the velocity distribution over an array, even under steered conditions. Methods for eliminating response notches, incorporating feedback and ABCD modeling were presented. Measured single element and array results substantiate the multiple resonance concept and modeling method. The results demonstrate that wideband performance can be obtained without unwanted cancellation between successive resonant frequencies.

ACKNOWLEDGEMENTS

We would like to thank FSI/Acoustikos, Cataumet, MA and John Baker who supervised fabrication and testing of the transducer element, array and feedback circuitry. We would also like to thank Jan F. Lindberg of ONR and NUWC, Newport, RI for his encouragement on this project. Work was performed under a Phase II SBIR Topic N01-103 and supported by ONR.

REFERENCES

[1] Patent Pending, J. L. Butler and A. L. Butler, Image Acoustics, Inc., Cohasset, MA, 02050

[2] Array interactive analysis program, ARRAY, Image Acoustics, Inc.

[3] Finite element program ANSYS, Ansys, Inc., Canonsburg, PA 15317

[4] Cascade matrix transducer design program, TRN, NUWC, Newport, RI., 02841

[5] Transducer circuit analysis program, TAP, Image Acoustics, Inc.